Supplementary Information for "Assessment of the Madden-Julian Oscillation in CMIP6 Models based on Moisture Mode Theory"

Qiao-Jun Lin[1], Víctor C. Mayta[1], and Ángel F. Adames Corraliza[1]

[1]Department of Atmospheric and Oceanic Sciences, University of Wisconsin, Madison, Wisconsin, USA

Contents of this file

1. MJO Phase speed: Radon Transform method

2. Parameters of N_{mode}

3. Figures S1, S2, S3, and S4

October 4, 2023, 7:32pm

1. MJO Phase speed: Radon Transform method

Following the previous studies (Yang et al., 2007; Mayta et al., 2021, 2023), the Radon Transform method (Radon, 1917) is adopted to objectively evaluate MJO phase speed based on the longitude-time plot (as shown in Fig. S1). The convective envelopes are projected onto a plate that has an angle θ ($0°$ to $180°$) relative to the x-axis (Fig. S2a), and the largest total amplitude $\sum_i P^2\left(x_i', \theta\right)$ will exist in θ_{max} (Fig. S2b). The phase speed can be estimated as

$$c_p = \frac{2\pi a \cos\psi}{360°} \tan(\theta_{max})\frac{\Delta x}{\Delta t} \tag{1}$$

where a is the earth's radius, and $\frac{2\pi a \cos\psi}{360°}$ is the length of unit degree at latitude ψ. The Δx and Δt are the temporal and spatial ($°$) resolutions of a data grid, respectively. Since the MJO propagation will accelerate when it crosses the Maritime Continent (Rushley et al., 2022), we only consider the range from $60°$E to $120°$E. For example, the c_p of ERA5 is $3.77\ ms^{-1}$ obtained from $\theta_{max} = 49.5°$ (Fig. S2b). The averaged c_p is $5.3 \pm 3.1\ ms^{-1}$ for 25 CMIP6 models, and 10 models simulate the $c_p > 5\ ms^{-1}$ (refer to Fig. S1). These results suggest that the MJO convection has a faster phase speed in model simulation than in the real world, consistent with the previous study of the MJO propagation in CMIP5 models (Ahn et al., 2017).

2. Parameters of N_{mode}

Here, we analyze whether the N_{mode} in the models is also sensitive to its phase speed. The equation of N_{mode} can be rewritten by common logarithm ($\log_{10}$)

$$\log_{10} N_{mode} \approx 2 \log_{10} c_p + \log_{10} \tau + (-\log_{10} \tau_c) + (-2 \log_{10} c) \tag{2}$$

Since the c is consistent ($= 50 \ ms^{-1}$), we neglect the last term. Figure S4 illustrates the scatterplots of the leading three terms in Eq. 2, including the slope (S) and correlation (R) to $\log_{10} N_{mode}$. For the 25 models, MJO phase speed has the highest relation with N_{mode} ($S = 1.37, R = 0.97$; Fig. S3a). Large and small N_{mode} values correspond to relatively fast and slow propagation, respectively. The temporal scale of wave shows a relatively weak effect and a negative correlation to N_{mode} ($S = -0.24, R = -0.79$; Fig. S3b). The contribution of $-\log_{10} \tau$ to $\log_{10} N_{mode}$ is much smaller than other terms ($S = -0.13, R = -0.54$; Fig. S3c). A high sensitivity of N_{mode} to c_p is also found in these 25 CMIP6 models, consistent with the observation in previous studies (e.g., Adames et al., 2019; Adames, 2022).
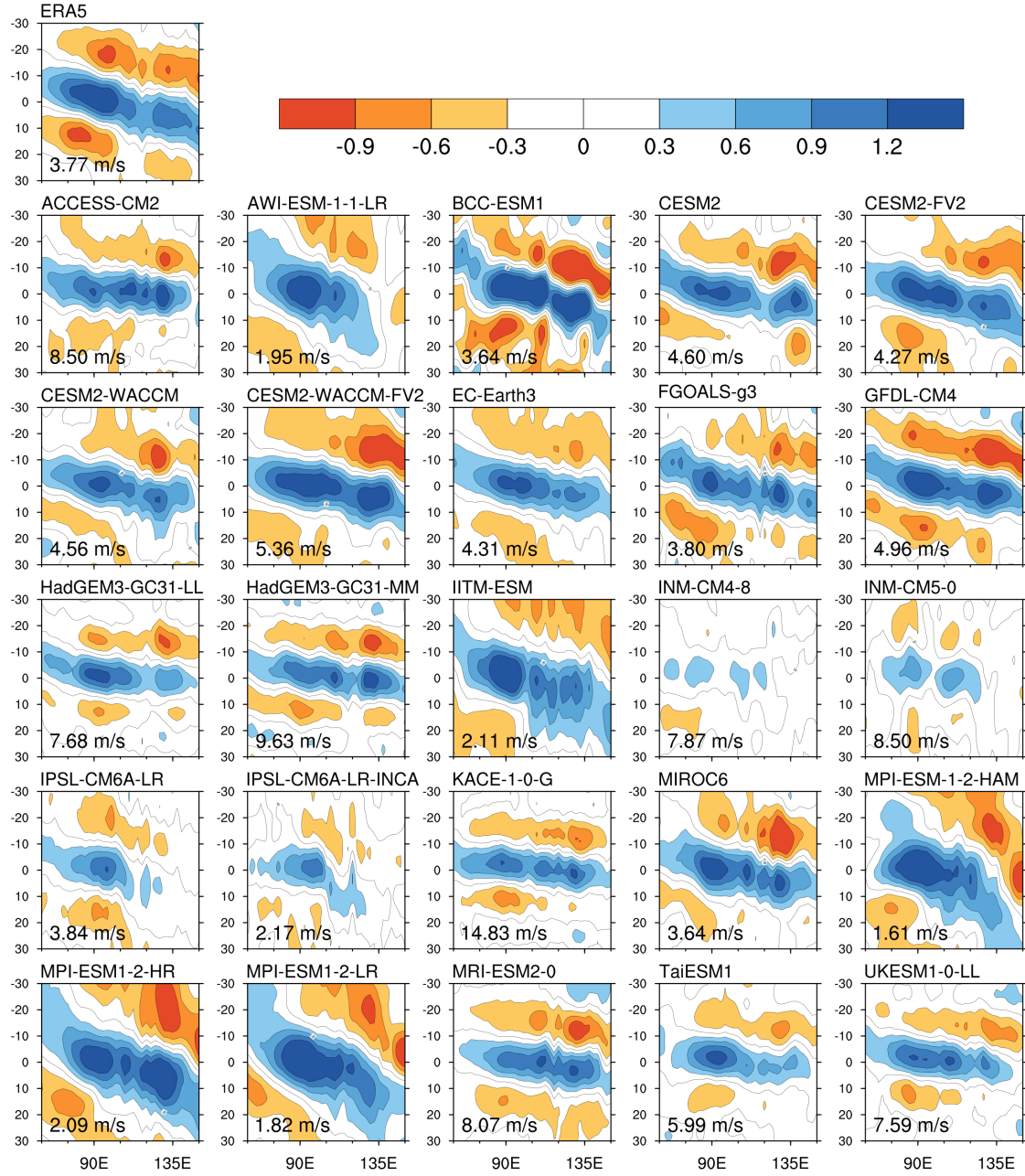
October 4, 2023, 7:32pm

Figure S1. Hovmöller diagram of regressed precipitation averaged between 10°S and 10°N from -30 to 30 days for the ERA5 and 25 CMIP6 models. Values in the bottom-left corner represent the MJO phase speed over 60°E-120°E calculated by using the Radon Transform. The contour interval is 0.3 mm day^{-1}.
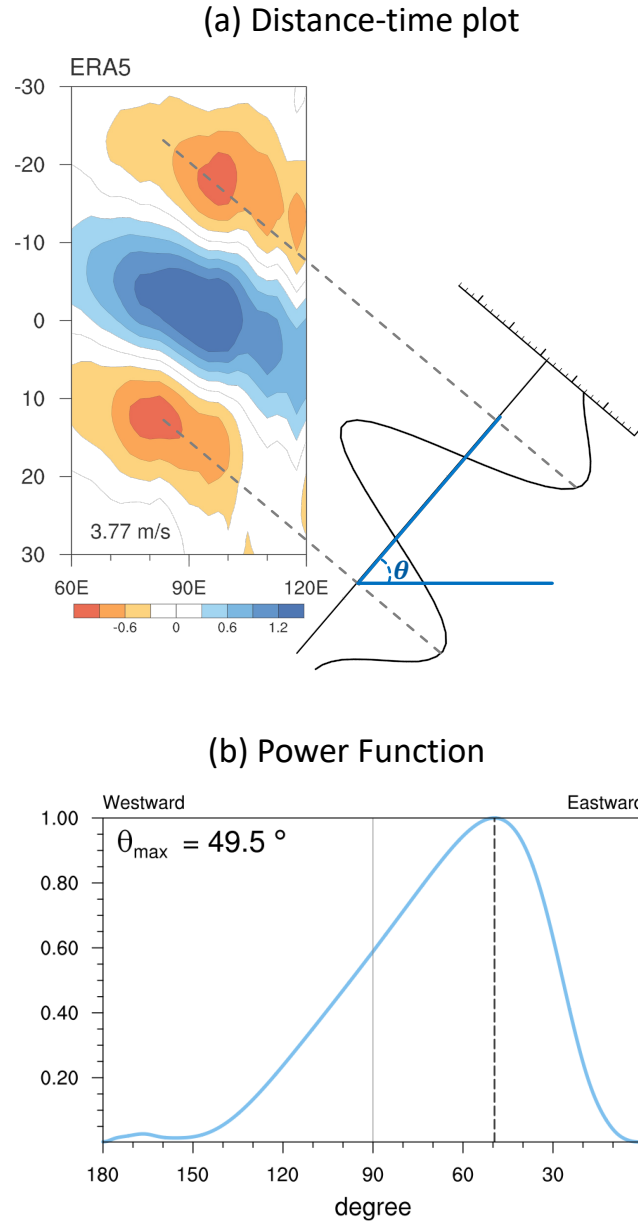
(a) Distance-time plot

ERA5

3.77 m/s

θ

-0.6   0   0.6   1.2

(b) Power Function

Westward   Eastward

θ_{max} = 49.5 °

180   150   120   90   60   30   0

degree

Figure S2. Schematic depicting the process of the Radon Transform method to estimate MJO phase speed in ERA5. (a) Hovmöller diagram projects onto a plate that has an angle θ with the x-axis. (b) The θ that has a maximum total absolute amplitude $\sum_i P^2 (x'_i, \theta)$ is defined as θ_{max}.
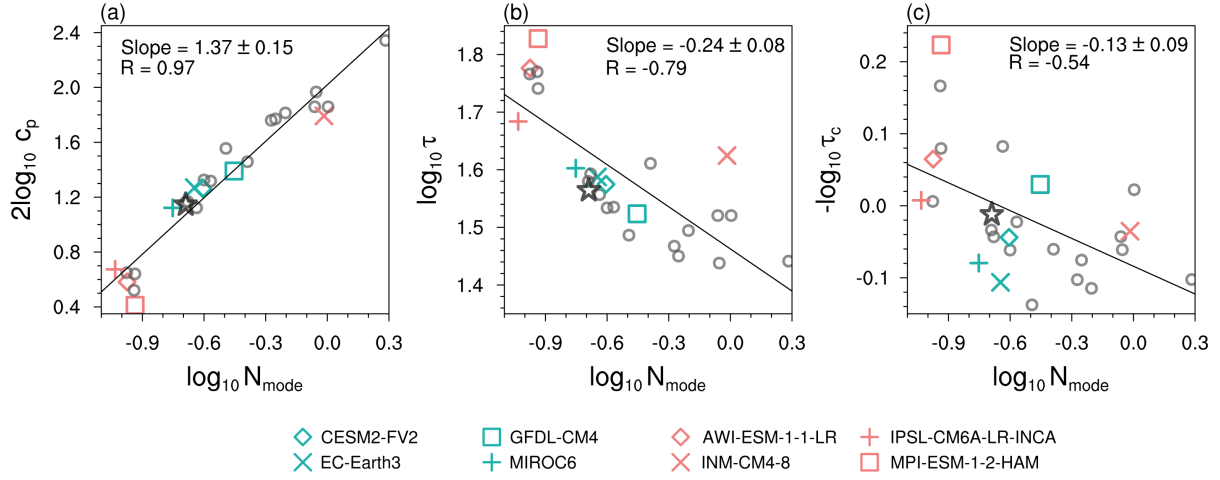
Figure S3. Scatterplot of (a) $2\log_{10} c_p$ (b) $\log_{10} \tau$, and (c) $-\log_{10} \tau_c$ versus $\log_{10} N_{mode}$ for

ERA5 (black star) and 25 CMIP6 models. The green and pink markers symbolize four good and

four poor models, respectively. Solid lines are calculated by the linear least-squares fitting. The

values in the top represent the slope of linear fits and correlation coefficient for 25 model results.

All correlation coefficients pass the 95% confidence interval (p-value < 0.05).

References

Adames, Á. F. (2022). The Basic Equations UnderWeak Temperature Gradient Balance: Formulation, Scaling, and Types of Convectively-coupled Motions. *Journal of the Atmospheric Sciences*.

Adames, Á. F., Kim, D., Clark, S. K., Ming, Y., & Inoue, K. (2019). Scale analysis of moist thermodynamics in a simple model and the relationship between moisture modes and gravity waves. *Journal of the Atmospheric Sciences*, *76*(12), 3863–3881.

Ahn, M.-S., Kim, D., Sperber, K. R., Kang, I.-S., Maloney, E., Waliser, D., & Hendon, H. (2017). MJO simulation in CMIP5 climate models: MJO skill metrics and process-oriented diagnosis. *Climate Dynamics*, *49*(11), 4023–4045.

Mayta, V. C., Adames Corraliza, Á. F., & Lin, Q.-J. (2023). The radon and hilbert transforms and their applications to atmospheric waves. *Atmospheric Science Letters*, *In Revision*(n/a).

Mayta, V. C., Kiladis, G. N., Dias, J., Silva Dias, P. L., & Gehne, M. (2021). Convectively coupled Kelvin waves over tropical South America. *Journal of Climate*, *34*(16), 6531–6547.

Radon, J. (1917). Uber die bestimmung von funktionen durch ihre intergralwerte la'ngs gewisser mannigfaltikeiten. *Ber. Sa'chsische Akad. Wiss*, 69–262.

Rushley, S. S., Janiga, M. A., Ridout, J. A., & Reynolds, C. A. (2022). The Impact of Mean State Moisture Biases on MJO Skill in the Navy ESPC. *Monthly Weather Review*.

Yang, G.-Y., Hoskins, B., & Slingo, J. (2007). Convectively coupled equatorial waves. Part II: Propagation characteristics. *Journal of the Atmospheric Sciences*, *64*(10), 3424–3437.